Progress In Electromagnetics Research, Vol. 105, 103–118, 2010

MICROWAVE SCATTERING AND ABSORPTION BY A MULTILAYERED LOSSY METAMATERIAL-GLASS CYLINDER

J. Bucinskas

Physics Department
Vilnius University
Vilnius, Lithuania

L. Nickelson and V. Sugurovas

Center for Physical Sciences and Technology
Semiconductor Physics Institute
A. Gostauto 11, Vilnius, Lithuania

Abstract—Here we present the rigorous electrodynamical solution of diffraction problem about the microwave scattering by a multilayered cylinder. The number and thickness of layers is not limited. We offer the solution when the central core of multilayered cylinder can be made of different isotropic materials as a metamaterial, a ceramic matter or a semiconductor as well as of a perfect metal. The isotropic coated layers can be of strongly lossy materials. The signs of the complex permittivity and complex permeability can be negative or positive in different combinations. Here we present dependencies of the scattered power of the incident perpendicularly and parallel polarized microwaves by the metamaterial-glass cylinder on signs of metamaterial permittivity as well as permeability. The glass layer absorbed power and metamaterial core absorbed power dependent on the hypothetic metamaterial permittivity and permeability signs at the wide range frequencies 1–120 GHz are also presented here. The metamaterial core of cylinder has a radius equal to 0.0018 m and the thickness of the coated acrylic-glass layer is 0.0002 m. We have found some conditions when the scattered-power has minimal values and the absorbed power by the coated acrylic glass layer is constant in a very wide frequency range. We have discovered that the glass layer absorbed power increases with increasing of the frequency at the range 1–120 GHz for both microwave polarizations.

Corresponding author: L. Nickelson (lucynickelson@gmail.com).

1. INTRODUCTION

For several decades scattering problems have been intensively analyzed. The importance of scattering problems is based on their great practical utility for many applications, such as reflector antennas, the analysis of structures in open space, electromagnetic (EM) defence of structures, the scattering modeling for remote sensing purposes, high frequency telecommunications, navigation, computer network, medicine, invisibility cloaks technology and radar systems. The stream of new scattering problem articles shows the actuality of the topic. EM scattering by dielectric and metal cylinders is a classical problem in EMs and has been investigated by many researchers [1–4]. An iterative algorithms based on the T-matrix approach for the EM scattering by dielectric cylinders with infinite and finite length is given in [1, 2]. The incident, scattered and transmitted fields are expressed in terms of the spherical harmonics in the T-matrix approach.

In paper [3], the computational results of radar cross-section for infinitely long conducting or dielectric circular cylinders with multilayer dielectric coatings are considered, where the number of dielectric layers may be arbitrary. TE, TM and circularly polarized normally incident plane waves were considered in that article. Paper [4] presents a hybrid method that was constructed by the finite-difference frequency domain and mode-matching methods for the analysis of EM wave scattering from some arbitrary cross-section metallic or dielectric cylinders.

Some scattering problems have created an enormous demand for modeling and simulation of cylinders with metamaterial layers [5–12]. The full wave iterative algorithm for the computation of the diffracted far field of the infinitely long cylinders that were coated with several dielectric layers is discussed in [5]. A cylindrical local basis function is used in the modal expansion of the diffraction operators. TE and TM polarized normally incident plane waves were considered. The hybrid algorithm that can be applied to a specific cases such as rotating and stationary metamaterial core coated with metallic or dielectric materials is given in [6]. The calculations were fulfilled for cylinders of lossless materials. An algorithm to study the scattering properties of multilayered metamaterial cylinders by the radiation of a line source is proposed in [7]. The algorithm is based on the eigenfunctional expansion. In [8] the EM scattering by a perfect circular cylinder conductor coated with a double positive (DP) material or a double negative (DN) material is investigated theoretically when the radiation source has a line form. The calculations were fulfilled for some lossless metamaterial cylinders.

Various methods have been developed to treat diffraction problems such as the T-matrix approach [1, 2], method of moments [5], Finite-difference time domain (FDTD) [10], Finite-difference frequency domain (FDFD) [4, 11], integral method [9] and method of partial areas [3, 7, 8].

Here we present the rigorous solution of the EM boundary problem. Our computer program let us take strongly dissipative materials of the layered cylinder. The proposed algorithm has no limitation on layers' thickness or their number. The algorithm is stable and effective. It enables one to investigate diffraction characteristics of complex composed cylinders even if the materials of nearby layers have opposite electric properties, and the sizes of the layers are very different.

Here we also present our numerical analyses of the scattered power as well as the absorbed powers by the coated acrylic-glass layer and the metamaterial core of two layered cylinder in the case of different signs of metamaterial complex permittivity and permeability components. The incident perpendicularly and parallel polarized microwaves are taken in the frequency range 1–120 GHz. The cylinder metamaterial core has the radius $R_2 = 0.0018$ m, and the external radius of the acrylic-glass layer is $R_1 = 0.002$ m.

Our numerical studies can be useful in solving at least two practical problems: a) for the correction of an antenna pattern, when the cylinder is placed in an antenna radiated field; b) to achieve the desired EM compatibility if there exists a problem of EM signal shielding from the interference with noise signals.

To solve these problems we have to investigate the dependence of scattered and absorbed powers on the signs of the metamaterial permittivity and permeability. In our work these signs are determined by values s_1, s_2, s_3, s_4. Our calculations were fulfilled when the permittivity was equal to $-\varepsilon' - i\varepsilon''$ (Re EPS is negative) at $s_1 = s_2 = -1$ or $\varepsilon' - i\varepsilon''$ (Re EPS is positive) at $s_1 = s_2 = 1$. And analogically the permeability was equal to $-\mu' - i\mu''$ at $s_3 = s_4 = -1$ or $\mu' - i\mu''$ at $s_3 = s_4 = 1$.

Many papers have reported the theoretical and experience development of metamaterials [12–19]. The variety of technologies for creation of engineering metamaterials increases rapidly. We do not introduce restrictions on the design elements of our hypothetical metamaterial and its aggregate state. Our hypothetical metamaterials can be liquid [14, 15], with alternating layers of metal and ceramic substrate [16], with ceramic inclusions [17], in the form of powder [18], ferromagnetic composites' inclusions [19], etc.

Analysis of articles on metamaterials shows that metamaterials

can be classified depending on the signs of their permittivity and permeability. In our work the double negative (DN) metamaterial is defined by values $s_1 = s_2 = s_3 = s_4 = -1$; double positive (DP) material [13] is determined by values $s_1 = s_2 = s_3 = s_4 = 1$; single negative metamaterial (SN) is defined by values $s_1 = s_2 = 1$, $s_3 = s_4 = -1$ or $s_1 = s_2 = -1$, $s_3 = s_4 = 1$. Each metamaterial is intended for use in a specific frequency range and has a specific value of the effective permittivity and permeability at each frequency. For this reason we took the absolute values of real and imaginary parts of permittivity and permeability constant at all frequencies. In this article we have focused our attention on choosing one type of metamaterials among DN (double negative) or DP (double positive) or SN (single negative) materials. We were guided only by the implementation of the correct electrodynamical solution when we select the signs of permittivity and permeability.

2. SCATTERING PROBLEM FORMULATION

Let us have an endless cylinder in the z-axis direction divided by surfaces $\rho = R_j$, $j = 1, \ldots, N$ in concentric regions. The j-th region ($R_{j+1} < \rho < R_j$, $j = 1, \ldots, N$) is filled with a material having the scalar permittivity ε_j and scalar permeability μ_j. Numbering of the layers is going from outside layer to the inner one. Thus R_1 is the outside radius of the cylinder and for $j > N$ the radius $R_{N+1} = 0$ (Fig. 1). The cylinder, put in medium with the permittivity ε and permeability μ, scatters a plane monochromatic EM wave. The electric field of the wave at the point $\vec{r}$ is $\vec{E}^{in}(\vec{r}) = \vec{E}_0 e^{\mathrm{i}\omega t - \mathrm{i}\vec{k}\vec{r}\sqrt{\varepsilon\mu}}$. Here $\vec{E}_0$ is the electric field vector of incident plane monochromatic EM wave that defines the wave polarization. ω is the EM wave frequency, and $\vec{k}$

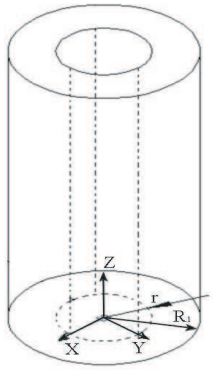

Figure 1. The simplest layered metamaterial cylinder model.

is the wave vector.

3. EXPRESSIONS OF MICROWAVE ELECTRIC FIELD IN LOSSY MEDIA

For harmonic waves the Maxwell's equations:

$$\nabla \times \vec{H} = \mathrm{i}\omega\varepsilon_0\varepsilon\vec{E}, \quad \nabla \times \vec{E} = -\mathrm{i}\omega\mu_0\mu\vec{H} \tag{1}$$

have solutions expressed by the transverse electric (TE) and magnetic (TM) waves in the cylinder coordinate system. After scalarization we get that TE and TM waves' potentials V_{TE} and V_{TM} satisfy the Helmholtz equations:

$$\frac{1}{\rho}\frac{\partial}{\partial\rho}\rho\frac{\partial V_{TM}}{\partial\rho} + \frac{1}{\rho^2}\frac{\partial^2 V_{TM}}{\partial\varphi^2} + \frac{\partial^2 V_{TM}}{\partial z^2} + k^2\varepsilon\mu V_{TM} = 0, \tag{2}$$

$$\frac{1}{\rho}\frac{\partial}{\partial\rho}\rho\frac{\partial V_{TE}}{\partial\rho} + \frac{1}{\rho^2}\frac{\partial^2 V_{TE}}{\partial\varphi^2} + \frac{\partial^2 V_{TE}}{\partial z^2} + k^2\varepsilon\mu V_{TE} = 0, \tag{3}$$

where ρ, φ, z are the radial, azimuthal and longitudinal coordinates. Here the value $k = \omega/c$ is the wavenumber of EM wave, and c is the speed of light in free space.

Their solutions are

$$\begin{aligned} V_{TM} = & \sum_{n=-\infty}^{\infty} \left(A_n^{(1)} H_n^{(1)} \left(\sqrt{k^2\varepsilon\mu - h^2}\rho \right) \right. \\ & \left. + A_n^{(2)} H_n^{(2)} \left(\sqrt{k^2\varepsilon\mu - h^2}\rho \right) \right) e^{in\varphi} e^{-ihz}, \end{aligned} \tag{4}$$

$$\begin{aligned} V_{TE} = & \sum_{n=-\infty}^{\infty} \left(B_n^{(1)} H_n^{(1)} \left(\sqrt{k^2\varepsilon\mu - h^2}\rho \right) \right. \\ & \left. + B_n^{(2)} H_n^{(2)} \left(\sqrt{k^2\varepsilon\mu - h^2}\rho \right) \right) e^{in\varphi} e^{-ihz}. \end{aligned} \tag{5}$$

Here $H_n^{(1)}(w)$ is the Hankel function of the n-th order and the first kind, and $H_n^{(2)}(w)$ is the Hankel function of the n-th order and the second kind. w is the argument $\left(\sqrt{k^2\varepsilon\mu - h^2}\rho \right)$ of functions, and h is the longitudinal propagation constant. $A_n^{(1)}$, $A_n^{(2)}$, $B_n^{(1)}$, $B_n^{(2)}$ are the unknown coefficients which must be determined. Outside the cylinder only the second kind Hankel function satisfies the radiation condition.

Thus for the scattering field we have

$$V_{TM} = \sum_{n=-\infty}^{\infty} A_n^s H_n^{(2)}(w)\ e^{in\varphi} e^{-ihz},$$

$$V_{TE} = \sum_{n=-\infty}^{\infty} B_n^s H_n^{(2)}(w)\ e^{in\varphi} e^{-ihz}. \tag{6}$$

In the regions $R_{j+1} < \rho < R_j$ $(j = 1, \ldots, N)$ there are inward an outward waves.

We can write schematically

$$V_{TMj} = V_{TMj}^{(1)} + V_{TMj}^{(2)}, \quad V_{TEj} = V_{TEj}^{(1)} + V_{TEj}^{(2)}. \tag{7}$$

Here the upper index shows the kind of the Hankel function. For the N-th region the solutions should be finite in the points $\rho = 0$. Therefore, one has to take Bessel function as radial functions. The EM field components are

$$E_\rho = \frac{\partial^2 V_{TM}}{\partial z \partial \rho} - \frac{i\omega\mu_0\mu}{\rho}\frac{\partial V_{TE}}{\partial \varphi}, \quad E_\varphi = \frac{1}{\rho}\frac{\partial^2 V_{TM}}{\partial z \partial \varphi} + i\omega\mu_0\mu\frac{\partial V_{TE}}{\partial \rho}, \tag{8}$$

$$E_z = -\frac{1}{\rho}\left\{\frac{\partial}{\partial \rho}\rho\frac{\partial V_{TM}}{\partial \rho} + \frac{\partial}{\partial \varphi}\frac{1}{\rho}\frac{\partial V_{TM}}{\partial \varphi}\right\}, \tag{9}$$

$$H_\rho = \frac{i\omega\varepsilon_0\varepsilon}{\rho}\frac{\partial V_{TM}}{\partial \varphi} + \frac{\partial^2 V_{TE}}{\partial z \partial \rho}, \quad H_\varphi = -i\omega\varepsilon_0\varepsilon\frac{\partial V_{TM}}{\partial \rho} + \frac{1}{\rho}\frac{\partial^2 V_{TE}}{\partial z \partial \varphi}, \tag{10}$$

$$H_z = -\frac{1}{\rho}\left\{\frac{\partial}{\partial \rho}\rho\frac{\partial V_{TE}}{\partial \rho} + \frac{\partial}{\partial \varphi}\frac{1}{\rho}\frac{\partial V_{TE}}{\partial \varphi}\right\}. \tag{11}$$

Here the constants ε_0 and μ_0 are the permittivity and permeability of free space.

The EM field in a cylinder layer is created by inward (the upper index (1)) and outward (the upper index (2)) waves. The whole field is made by some vector sums of these fields. In the j-th cylinder layer

($R_{j+1} \le \rho \le R_j$) Fourier-components with respect to z-coordinate are:

$$E_\rho^j = \left[\mathrm{i}h \sum_{m=-\infty}^{\infty} B_{jm}^{(1)} \frac{\partial H_m^{(1)}(\beta_j\rho)}{\partial\rho} + \frac{\omega\mu_0\mu_j}{\rho} \sum_{m=-\infty}^{\infty} mA_{jm}^{(1)} H_m^{(1)}(\beta_j\rho) \right] e^{im\varphi}$$
$$+ \left[\mathrm{i}h \sum_{m=-\infty}^{\infty} B_{jm}^{(2)} \frac{\partial H_m^{(2)}(\beta_j\rho)}{\partial\rho} + \frac{\omega\mu_0\mu_j}{\rho} \sum_{m=-\infty}^{\infty} mA_{jm}^{(2)} H_m^{(2)}(\beta_j\rho) \right] e^{im\varphi}, \quad (12)$$

$$E_\varphi^j = \left[-\frac{h}{\rho} \sum_{m=-\infty}^{\infty} mB_{jm}^{(1)} H_m^{(1)}(\beta_j\rho) + \mathrm{i}\omega\mu_0\mu_j \sum_{m=-\infty}^{\infty} A_{jm}^{(1)} \frac{\partial H_m^{(1)}(\beta_j\rho)}{\partial\rho} \right] e^{im\varphi}$$
$$+ \left[-\frac{h}{\rho} \sum_{m=-\infty}^{\infty} mB_{jm}^{(2)} H_m^{(2)}(\beta_j\rho) + \mathrm{i}\omega\mu_0\mu_j \sum_{m=-\infty}^{\infty} A_{jm}^{(2)} \frac{\partial H_m^{(2)}(\beta_j\rho)}{\partial\rho} \right] e^{im\varphi}, \quad (13)$$

$$E_z^j = \beta_j^2 \sum_{m=-\infty}^{\infty} B_{jm}^{(1)} H_m^{(1)}(\beta_j\rho)\, e^{im\varphi} + \beta_j^2 \sum_{m=-\infty}^{\infty} B_{jm}^{(2)} H_m^{(2)}(\beta_j\rho)\, e^{im\varphi}, \quad (14)$$

$$H_\rho^j = \left[-\frac{\omega\varepsilon_0\varepsilon_j}{\rho} \sum_{m=-\infty}^{\infty} mB_{jm}^{(1)} H_m^{(1)}(\beta_j\rho) + \mathrm{i}h \sum_{m=-\infty}^{\infty} A_{jm}^{(1)} \frac{\partial H_m^{(1)}(\beta_j\rho)}{\partial\rho} \right] e^{im\varphi}$$
$$+ \left[-\frac{\omega\varepsilon_0\varepsilon_j}{\rho} \sum_{m=-\infty}^{\infty} mB_{jm}^{(2)} H_m^{(2)}(\beta_j\rho) + \mathrm{i}h \sum_{m=-\infty}^{\infty} A_{jm}^{(2)} \frac{\partial H_m^{(2)}(\beta_j\rho)}{\partial\rho} \right] e^{im\varphi}, \quad (15)$$

$$H_\varphi^j = \left[-\mathrm{i}\omega\varepsilon_0\varepsilon_j \sum_{m=-\infty}^{\infty} B_{jm}^{(1)} \frac{\partial H_m^{(1)}(\beta_j\rho)}{\partial\rho} - \frac{h}{\rho} \sum_{m=-\infty}^{\infty} mA_{jm}^{(1)} H_m^{(1)}(\beta_j\rho) \right] e^{im\varphi}$$
$$+ \left[-\mathrm{i}\omega\varepsilon_0\varepsilon_j \sum_{m=-\infty}^{\infty} B_{jm}^{(2)} \frac{\partial H_m^{(2)}(\beta_j\rho)}{\partial\rho} - \frac{h}{\rho} \sum_{m=-\infty}^{\infty} mA_{jm}^{(2)} H_m^{(2)}(\beta_j\rho) \right] e^{im\varphi}, \quad (16)$$

$$H_z^j = \beta_j^2 \sum_{m=-\infty}^{\infty} A_{jm}^{(1)} H_m^{(1)}(\beta_j\rho) e^{im\varphi} + \beta_j^2 \sum_{m=-\infty}^{\infty} A_{jm}^{(2)} H_m^{(2)}(\beta_j\rho) e^{im\varphi}. \quad (17)$$

To solve the scattering problem we use the standard boundary conditions, i.e., equality of the tangential EM field components. For the outside surface $\rho = R_1$ we have the expressions:

$$\left\{ E_z^s + E_z^{in} - E_{1,z}^{tr} \right\}\Big|_{\rho=R_1} = 0, \quad \left\{ E_\varphi^s + E_\varphi^{in} - E_{1,\varphi}^{tr} \right\}\Big|_{\rho=R_1} = 0, \quad (18)$$

$$\left\{ H_z^s + H_z^{in} - H_{1,z}^{tr} \right\}_{\rho=R_1} = 0, \quad \left\{ H_\varphi^s + H_\varphi^{in} - H_{1,\varphi}^{tr} \right\}_{\rho=R_1} = 0, \quad (19)$$

where E_z^{in}, E_φ^{in}, H_z^{in}, H_φ^{in} are the electric and magnetic tangential components of incident wave EM field, and E_z^s, E_φ^s, H_z^s, H_φ^s are the

electric and magnetic tangential components of scattered wave EM field. E_z^{tr}, E_φ^{tr}, and H_z^{tr}, H_φ^{tr} are the electric and magnetic tangential components of transmitted wave EM field.

For the inner surfaces $\rho = R_j$, $j = 2, \ldots, N$ the boundary conditions are:

$$\{E_{j,z} - E_{j-1,z}\}|_{\rho=R_j} = 0, \qquad \{E_{j,\varphi} - E_{j-1,\varphi}\}|_{\rho=R_j} = 0, \tag{20}$$

$$\{H_{j,z} - H_{j-1,z}\}_{\rho=R_j} = 0, \qquad \{H_{j,\varphi} - H_{j-1,\varphi}\}_{\rho=R_j} = 0. \tag{21}$$

The system of the boundary conditions on the outside surface $\rho = R_1$ for cylinder with N layers is:

$$\begin{aligned} &-\beta^2 B_m^s H_m^{(2)}(\beta R_1) + \beta_1^2 B_{1m}^{(1)} H_m^{(1)}(\beta_1 R_1) + \beta_1^2 B_{1m}^{(2)} H_m^{(2)}(\beta_1 R_1) \\ &= E_{0z}\sqrt{2\pi}\delta(h + k_z\sqrt{\varepsilon\mu})(-\mathrm{i})^m J_m(\beta R_1), \end{aligned} \tag{22}$$

$$\begin{aligned} &-\beta^2 A_m^s H_m^{(2)}(\beta R_1) + \beta_1^2 A_{1m}^{(1)} H_m^{(1)}(\beta_1 R_1) + \beta_1^2 A_{1m}^{(2)} H_m^{(2)}(\beta_1 R_1) \\ &= H_{0z}\sqrt{2\pi}\delta(h + k_z\sqrt{\varepsilon\mu})(-\mathrm{i})^m J_m(\beta R_1), \end{aligned} \tag{23}$$

$$\begin{aligned} &-\mathrm{i}\omega\mu_0\mu A_m^s \frac{\partial H_m^{(2)}(\beta R_1)}{\partial R_1} + \frac{hm}{R_1} B_m^s H_m^{(2)}(\beta R_1) \\ &+\mathrm{i}\omega\mu_0\mu_1 A_{1m}^{(1)} \frac{\partial H_m^{(1)}(\beta_1 R_1)}{\partial R_1} - \frac{hm}{R_1} B_{1m}^{(1)} H_m^{(1)}(\beta_1 R_1) \\ &+\mathrm{i}\omega\mu_0\mu_1 A_{1m}^{(2)} \frac{\partial H_m^{(2)}(\beta_1 R_1)}{\partial R_1} - \frac{hm}{R_1} B_{1m}^{(2)} H_m^{(2)}(\beta_1 R_1) \\ &= \sqrt{2\pi}\delta(h + k_z\sqrt{\varepsilon\mu})(-\mathrm{i})^m \left(\mathrm{i}E_{0y} \frac{\partial J_m(\beta R_1)}{\partial(\beta R_1)} - E_{0x} \frac{m}{\beta R_1} J_m(\beta R_1)\right), \end{aligned} \tag{24}$$

$$\begin{aligned} &\frac{hm}{R_1} A_m^s H_m^{(2)}(\beta R_1) + \mathrm{i}\omega\varepsilon_0\varepsilon B_m^s \frac{\partial H_m^{(2)}(\beta R_1)}{\partial R_1} \\ &-\frac{hm}{R_1} A_{1m}^{(1)} H_m^{(1)}(\beta_1 R_1) - \mathrm{i}\omega\varepsilon_0\varepsilon_1 B_{1m}^{(1)} \frac{\partial H_m^{(1)}(\beta_1 R_1)}{\partial R_1} \\ &-\frac{hm}{R_1} A_{1m}^{(2)} H_m^{(2)}(\beta_1 R_1) - \mathrm{i}\omega\varepsilon_0\varepsilon_1 B_{1m}^{(2)} \frac{\partial H_m^{(2)}(\beta_1 R_1)}{\partial R_1} \\ &= \sqrt{2\pi}\delta(h + k_z\sqrt{\varepsilon\mu})(-\mathrm{i})^m \left(\mathrm{i}H_{0y} \frac{\partial J_m(\beta R_1)}{\partial(\beta R_1)} - H_{0x} \frac{m}{\beta R_1} J_m(\beta R_1)\right). \end{aligned} \tag{25}$$

Here $\beta_j^2 = k^2\varepsilon_j\mu_j - h^2$, β_j is the transversal wave number in the layer j, and $\beta^2 = k^2\varepsilon\mu - h^2$, β is the transversal wave number in a cylinder surrounding media space. The values of $\sqrt{\beta^2}$ are chosen in standard way. We write $\beta^2 = |\beta|^2 \exp(i\alpha)$, $-\pi \succ \alpha \prec \pi$. If $-\pi \succ \alpha \prec 0$

then $\beta = |\beta| \exp\,(i\alpha/2)$. The function $H^{(2)}(\beta\rho)$ at infinity $\rho \to \infty$ disappears. If $\pi \succ \alpha \succ 0$ one has to take for the root another value $\beta = -|\beta| \exp(i\alpha/2)$. Then the function $H^{(2)}(\beta\rho)$ disappears at infinity $\rho \to \infty$ again. The value $\vec{H}_0 = \sqrt{\frac{\varepsilon_0\varepsilon}{\mu_0\mu}}\,\left[\vec{k}_0, \vec{E}_0\right]$, here the vectors $\vec{H}_0$ are the magnetic fields of the plane monochromatic incident EM wave (microwave), $\vec{E}_0 = E_{0x}\vec{n}_x + E_{0y}\vec{n}_y + E_{0z}\vec{n}_z$, where magnitudes E_{0x}, E_{0y}, E_{0z} are components of electric field $\vec{E}_0$, and the magnitudes H_{0x}, H_{0y}, H_{0z} are components of magnetic field $\vec{H}_0$. $\vec{k}_0 = \vec{k}/k$ is the unit vector, and the wave vector $\vec{k} = k_x\vec{n}_x + k_z\vec{n}_z$. $\vec{n}_x$, $\vec{n}_y$, $\vec{n}_z$ are the Cartesian coordinate system orts, and $J_m(\beta\rho)$ is the cylindrical Bessel function of the m-th order. The index m are also from $-\infty$ to $+\infty$, and $\delta(h + k_z\sqrt{\varepsilon\mu})$ is the Dirac delta function.

We can write the boundary conditions in the analogical way for the case when $\rho = R_N$ and $\rho = R_j$, $j = 2, \ldots, N-1$. We obtain the final system of equations from all the boundary conditions. From this equation system one gets the unknown coefficients as $A^{(1)}_{jm}$, $B^{(1)}_{jm}$, $A^{(2)}_{jm}$, $B^{(2)}_{jm}$. The Poynting vector describes energy flux, and it is equal to

$$\vec{P} = \left[\vec{E}, \vec{H}^*\right]. \tag{26}$$

Bearing in mind the EM fields' harmonic dependence on time after taking mean of (26) one obtains the factor 0.5. In Formulas (12)–(17) one has to use amplitudes of the fields. Integrating over surface of unit length cylinder with radius ρ we find the scattered or absorbed powers:

$$W = \frac{1}{2}\int\limits_0^{2\pi} \left(\vec{P}\vec{n}_\rho\right) \rho \mathrm{d}\varphi, \tag{27}$$

here $\vec{n}_\rho$ is the cylindrical coordinate system ort.

After having done some algebra one gets the power absorbed and

scattered by the cylinder:

$$W = \pi \sum_{m=-\infty}^{\infty} \left\{ \left[-hm \left(B_m^{(1)} H_m^{(1)} + B_m^{(2)} H_m^{(2)} \right) \right.\right.$$
$$\left. + \mathrm{i}\omega\mu_0\mu\rho \left(A_m^{(1)} \frac{\partial H_m^{(1)}}{\partial \rho} + A_m^{(2)} \frac{\partial H_m^{(2)}}{\partial \rho} \right) \right]$$
$$\beta^{2^*} \left(A_m^{(1)^*} H_m^{(1)^*} + A_m^{(2)^*} H_m^{(2)^*} \right) - \beta^2 \left(B_m^{(1)} H_m^{(1)} + B_m^{(2)} H_m^{(2)} \right) \qquad (28)$$
$$\left[\mathrm{i}\omega\varepsilon_0\varepsilon\rho \left(B_m^{(1)^*} \frac{\partial H_m^{(1)^*}}{\partial \rho} + B_m^{(2)^*} \frac{\partial H_m^{(2)^*}}{\partial \rho} \right) \right.$$
$$\left. \left. - h^* m \left(A_m^{(1)^*} H_m^{(1)^*} + A_m^{(2)^*} H_m^{(2)^*} \right) \right] \right\},$$

when we calculate the scattered power by Formula (28) then coefficients $A_m^{(1)}$, $A_m^{(1)^*}$, $B_m^{(1)}$, $B_m^{(1)^*}$ became equal to zero, and asterisks near magnitudes mean the conjugate values of these magnitudes. The argument of radial functions is $\beta\rho$ when $\rho \geq R_1$ and $\beta_j\rho$ when $R_{j+1} < \rho \leq R_j$.

4. NUMERICAL ANALYSIS OF THE REFLACTON AND ABSORBTION MICROWAVE POWER OF LAYERED METAMATERIAL-GLASS CYLINDER

In this section, we investigate the scattered and absorbed powers of the incident microwave by the layered metamaterial-glass cylinder in the frequency range from 1 till 120 GHz. The maximum number of members m in the sums of formulae was taken equal to 24 in our calculations. The metamaterial core of the layered cylinder is coated with some acrylic-glass. The external cylinder radius is $R_1 = 0.002\,\mathrm{m}$, and the cylinder core has radius $R_2 = 0.0018\,\mathrm{m}$, so the thickness of the glass layer is 0.0002 m. The acrylic-glass complex permittivity is $\varepsilon_g = \varepsilon_g' - \mathrm{i}\varepsilon_g'' = 3.8 - i0.0005$, $\varepsilon_g = |\varepsilon_g| \exp(-i\delta_\varepsilon^g)$, i.e., the phase of the complex glass permittivity is $\delta_\varepsilon^g = \arctan\left(\varepsilon_g''/\varepsilon_g'\right) \approx 1.3 \cdot 10^{-4}$ [rad], and the glass permeability is equal to $\mu_g = 1$.

Nowadays, there is great interest in the composite materials with untraditional values of the complex permittivity ε_{met} and complex permeability μ_{met}. We analyze here the scattered (reflected) and absorbed powers for four versions of hypothetic metamaterial parameter signs. The complex metamaterial permittivity $\varepsilon_{met} = s_1 |\varepsilon_{met}| \exp(-s_2 i\delta_\varepsilon^{met})$ was taken for two combinations of signs, when $s_1 = s_2 = \pm 1$. The complex metamaterial permeability $\mu_{met} =$

$s_3 |\mu_{met}| \exp(-s_4 i \delta_\mu^{met})$ was also taken for two combinations of signs, viz. $s_3 = s_4 = \pm 1$. The magnitude δ_ε^{met} is a phase of the complex permittivity ε_{met}, and the magnitude δ_μ^{met} is a phase of the complex permeability μ_{met}. Values of our hypothetic metamaterial permittivity and permeability components were taken $|\varepsilon_{met}| = 20$, $\delta_\varepsilon^{met} = 0.7068$ [rad] and $|\mu_{met}| = 2$ $\delta_\mu^{met} = 0.6283$ [rad]. These components were constant at all frequencies for reason mentioned in the end of the first section.

How the signs of the complex metamaterial permittivity and permeability influence the scattered and absorbed powers, when the plane perpendicularly $\vec{E}_0^{in} \perp \vec{n}_z$ or parallel $\vec{E}_0^{in} \| \vec{n}_z$ polarized microwave impinges on the layered metamaterial-glass cylinder (Fig. 1), is analyzed in Figs. 2–7. The normalized scattered or absorbed power values per oscillation period for the unit length of the two-layered metamaterial-glass cylinder are presented in these figures.

The absorbed and scattered power calculations were fulfilled using formula (28). The integral (28) has a positive sign when we calculate the scattered power. And this integral (28) has a negative sign when we calculate the absorbed power. For this reason, the scattered power has a positive value, and the absorbed power has a negative one (see Figs. 2–7). In our calculations the value is $|\vec{E}_0| = 1$. Designations in Figs. 2–7 correspond: curve 1 is for a DP material when $s_1 = s_2 = s_3 = s_4 = +1$ (line with black squares); curve 2 is for a SN material when $s_1 = s_2 = +1$, $s_3 = s_4 = -1$ (line with empty squares); curve 3 is for a SN material when $s_1 = s_2 = -1$, $s_3 = s_4 = +1$ (line with black triangulars); curve 4 is for a DN material when $s_1 = s_2 = s_3 = s_4 = -1$ (line with empty triangulars).

The diffraction dependence of the layered metamaterial-glass

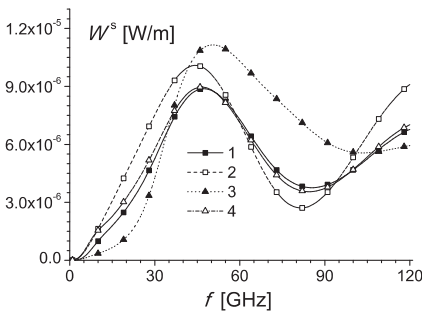

Figure 2. Scattered power dependencies on the frequency of incident perpendicularly polarized microwave.

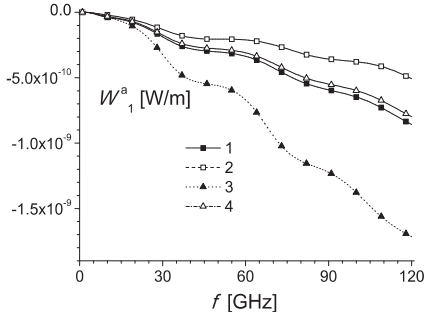

Figure 3. Dependencies of absorbed by glass layer power on the frequency of incident perpendicularly polarized microwave.

waveguide when the incident microwave has a perpendicular polarization $\vec{E}_0^{in} \perp \vec{n}_z$ is shown in Figs. 2–4. The dependence of scattered power W^s on the microwave frequency f is presented in Fig. 2. We see that the character of the curves for all metamaterial sign versions (curves 1–4) is the same. A comparison of curves 1–4 shows that only curve 3 that describes the metamaterial permittivity and permeability signs $s_1 = s_2 = -1$, $s_3 = s_4 = +1$ is the most different one compared with the other three cases. At the beginning, the scattered power grows till the maximum value, after that decreases till the minimum and later increases again with increasing frequency. So the dependence of magnitude $W^s = W^s(|f|)$ has a strong wave behavior. The scattered power maximums of all curves are in the frequency range about 44–52 GHz. Curves 1 and 4 practically coincide with each other. The lowest scattered power is for curve 3 at the frequencies about 1–35 GHz, and the scattered power minimum exists for curve 2 approximately at frequency 80 GHz.

Fig. 3 presents the absorbed microwave power W_1^a by the coated glass layer. The behavior of the microwave power absorption strongly depends on the permittivity and permeability signs s_1, s_2, s_3, s_4. The absorption is especially different at the higher frequencies. The absorption power of the glass layer is larger at higher frequencies.

The absorbed power W_1^a is the lowest when the metamaterial permittivity has some positive values of real part, and the permeability has some negative value (curve 2). The behavior of $W_1^a(|f|)$ is especially different for the third case when $s_1 = s_2 = -1$, $s_3 = s_4 = +1$ (Fig. 3). The absorption by the coated glass layer is the largest, when the SN metamaterial permittivity has some negative values, and the permeability has some positive ones (curve 3). In Fig. 3 curves 1 and 4 practically coincide.

Fig. 4 gives the absorbed power by the metamaterial core of the cylinder. We see that the W_2^a magnitudes have the pronounced wave-like nature dependent on the frequency. The metamaterial core absorption is the largest when the metamaterial permittivity has some negative values, and the permeability has some positive values (curve 3).

The diffraction dependence of the layered metamaterial-glass waveguide when the incident microwave has a parallel polarization $\vec{E}_0^{in} || \vec{n}_z$ is shown in Figs. 5–7. Fig. 5 presents the scattered power dependence on the frequency.

The scattered power dependence of the incident perpendicularly polarized wave (Fig. 2) and incident parallel polarized microwave (Fig. 5) are different. The scattered microwave power curves for the incident parallel polarized microwave have two maximums in the

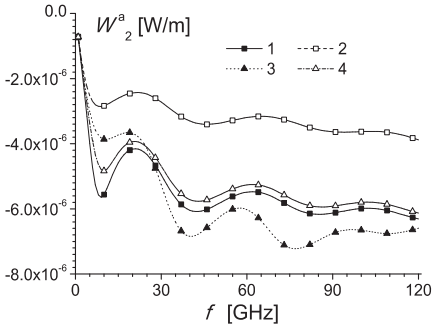

Figure 4. Dependencies of absorbed by metamaterial core power on the frequency of incident perpendicularly polarized microwave.

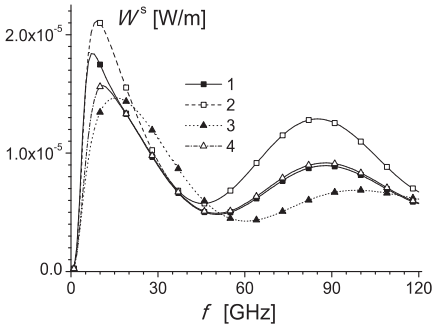

Figure 5. Scattered power dependencies on the frequency of incident parallel polarized microwave.

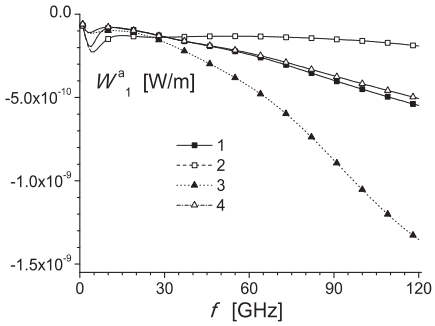

Figure 6. Dependencies of absorbed by coated glass layer power on the frequency of incident parallel polarized microwave.

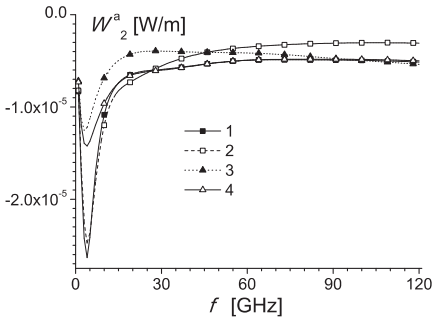

Figure 7. Dependencies of absorbed by metamaterial core power on the frequency of incident parallel polarized microwave.

frequency range 1–120 GHz. While the scattered power curves for the incident perpendicularly polarized microwave have only one maximum in the same frequency range (Fig. 2).

The first and second maximums of W^s in Fig. 5 are approximately in frequency intervals 10–20 GHz and 85–100 GHz. The largest scattering is at the lower frequencies. The maximum scattering is higher for the incident parallel polarized microwave in comparison with the incident perpendicularly polarized one. Fig. 6 presents the absorbed power by the coated glass layer for the incident parallel polarized microwave.

There are some small distortion "hooks" of the absorbed power at

the low frequencies. The absorbed power by glass layer increases with increasing frequencies (curves 1, 3, 4) for frequencies that are larger than 20 GHz. The absorbed power $W_1^a(|f|)$ is approximately constant when the SN metamaterial core permittivity and permeability have signs $s_1 = s_2 = +1$, $s_3 = s_4 = -1$.

Fig. 7 gives the metamaterial core absorbed power W_2^a for the incident parallel polarized microwave. We see that the absorbed-powers have the maximum values at about 5 GHz, and their values vary slightly after 20 GHz with increasing frequency. The absorption by the metamaterial is the largest at low frequencies (curves 1 and 2) when the metamaterial has the positive permittivity. The comparison of absorbed powers in Figs. 4 and 7 shows that dependencies are absolutely different.

We see that curves 1 and 4 in Figs. 2–7 are located very close to each other. The signs of the permittivity and permeability corresponding to these curves are opposite. Since the permittivity and permeability are located in unequal terms of boundary conditions (for example, see Equations (24), (25)). For this reason, the coincidence of curves 1 and 4 at some frequencies is not mandatory.

One of our numerical research goals was comparing diffraction characteristics when the cylinder core has the permittivity and permeability as some DN, SN or DP materials. We see that at some frequencies the characteristics can be different.

5. CONCLUSIONS

- We present here the simple effective algorithm that let us analyze diffraction characteristics of the multilayered cylinder of different strongly lossy or lossless isotropic materials. The number and size of cylinder layers are not limited.
- We presents here numerical calculations of the scattered power, absorbed powers by coated acrylic-glass layer and by the metamaterial core, their dependencies on wave polarization, on the signs of metamaterial complex permittivity and permeability components (Figs. 2–7).
- We found that the scattered power's dependence has wave behaviors. The minimal scattering from the metamaterial-glass cylinder is observed for the every metamaterial with some sign combinations of the permittivity and permeability at the special frequency range (Figs. 2 and 5).
- We found that the largest absorbed power by the coated acrylic-glass layer is observed for the case when the metamaterial is a

single negative material with the negative permittivity. The absorbed power of the glass layer increases with increasing frequency in the range 1–120 GHz for both microwave polarizations (Figs. 3 and 6).

- The metamaterial core absorbed power of the parallel polarized incident microwave has the minimum value at low frequencies and slightly dependent on the frequency at the range 20–120 GHz (Fig. 7).

REFERENCES

1. Yan, W.-Z., Y. Du, H. Wu, D. W. Liu, and B.-I. Wu, "EM scattering from a long dielectric circular cylinder," *Progress In Electromagnetics Research*, Vol. 85, 39–67, 2008.
2. Yan, W.-Z., Y. Du, Z. Li, E. Chen, and J. Shi, "Characterization of the validity region of the extended T-matrix method for scattering from dielectric cylinders with finite length," *Progress In Electromagnetics Research*, Vol. 96, 309–328, 2009.
3. Oraizi, H. and A. Abdolali, "Ultra wide band RCS optimization of multilayered cylindrical structures for arbitrarily polarized incident plane waves," *Progress In Electromagnetics Research*, Vol. 78, 129–157, 2008.
4. Kusiek, A. and J. Mazur, "Analysis of scattering from arbitrary configuration of cylindrical objects using hybrid finite-difference mode-matching method," *Progress In Electromagnetics Research*, Vol. 97, 105–127, 2009.
5. Hatamzadeh-Varmazyar, S., M. Naser-Moghadasi, and Z. Masouri, "A moment method simulation of electromagnetic scattering from conducting bodies," *Progress In Electromagnetics Research*, Vol. 81, 99–119, 2008.
6. Qiu, C.-W., S. Zouhdi, and Y. L. Geng, "Shifted resonances in coated metamaterial cylinders: Enhanced backscattering and near-field effects," *Physical Review E*, Vol. 77, 046604-(1-9), 2008.
7. Qiu, C.-W., H.-Y. Yao, S.-N. Burokur, S. Zouhdi, and L.-W. Li, "Electromagnetic scattering properties in a multilayered metamaterial cylinder," *IEICE Transactions Commun. E Series B*, Vol. 90, No. 9, 2423–2429, 2007.
8. Ahmed, S. and Q. A. Naqvi, "Directive EM radiation of a line source in the presence of a coated PEMC circular cylinder," *Progress In Electromagnetics Research*, Vol. 92, 91–102, 2009.
9. Nickelson, L. and V. Shugurov, *Singular Integral Equations'*

Methods for the Analysis of Microwave Structures, 348, VSP Brill Academic Publishers, Leiden-Boston, 2005.

10. Rogier, H., "A new hybrid FDTD-BIE approach to model electromagnetic scattering problems," *IEEE Microwave and Guided Wave Letters*, Vol. 8, No. 3, 138–140, 1998.
11. Sharkawy, M. A., V. Demir, and A. Z. Elsherbeni, "Plane wave scattering from three dimensional multiple objects using the iterative multiregion technique based on the FDFD method," *IEEE Trans. on AP*, Vol. 54, No. 2, 666–673, 2006.
12. Penciu, R. S., M. Kafesaki, T. F. Gundogdu, E. N. Economou, and C. M. Soukoulis, "Theoretical study of left-handed behavior of composite metamaterials," *Photonics Nanostructures Fundamentals and Applications*, Vol. 4, No. 1, 12–16, Elsevier, 2006.
13. Kim, K. Y. "Comparative analysis of guided modal properties of double-positive and double-negative metamaterial slab waveguides," *Radioengineering*, Vol. 18, No. 2, 117–123, 2009.
14. Pratibha, R., K. Park, I. Smalyukh, and W. Park, "Tunable optical metamaterial based on liquid crystal-gold nanosphere composite," *Optics. Express*, Vol. 17, No. 22, 19459–19469, 2009.
15. Zhang, F., Q. Zhao, D. P. Gaillot, X. Zhao, and D. Lippens, "Numerical investigation of metamaterials infiltrated by liquid crystal," *Journal of the Optical Society of America B*, Vol. 25, No. 11, 1920–1925, 2008.
16. Du, B., J. Zhou, and L. F. Hao, "Fabrication and properties of meta-materials based on multilayer ceramic structure," *Journal of Electroceramics*, Vol. 21, No. 1–4, 165–169, 2008.
17. Schuller, J. A., R. Zia, T. Taubner, and M. L. Brongersma, "Dielectric metamaterials based on electric and magnetic resonances of silicon carbide particles," *Physical Review Letters*, Vol. 99, 107401-(1-4), 2007.
18. Adenot-Engelvin, A. L., C. Dudek, P. Toneguzzo, and O. Acher, "Microwave properties of ferromagnetic composites and metamaterials," *Journal of the European Ceramic Society*, Vol. 27, No. 2–3, 1029–1033, 2007.
19. Vázquez, M. and A.-L. Adenot-Engelvin, "Glass-coated amorphous ferromagnetic microwires at microwave frequencies," *Journal of Magnetism and Magnetic Materials*, Vol. 321, No. 14, 2066–2073, 2009.